Using Growing Cell Structures for Surface Reconstruction

I.P. Ivrissimtzis W-K. Jeong H-P. Seidel

Max-Plank-Institut für Informatik, Stuhlsatzenhausweg 85,
Saarbrücken, D-66123, Germany
{ivrissimtzis, jeong, hpseidel}@mpi-sb.mpg.de

Abstract

We study the use of neural network algorithms in surface reconstruction from an unorganized point cloud, and meshing of an implicit surface. We found that for such applications, the most suitable type of neural networks is a modified version of the Growing Cell Structure we propose here. The algorithm works by sampling randomly a target space, usually a point cloud or an implicit surface, and adjusting accordingly the neural network. The adjustment includes the connectivity of the network. Doing several experiments we found that the algorithm gives satisfactory results in some challenging situations involving sharp features and concavities. Another attractive feature of the algorithm is that its speed is virtually independent from the size of the input data, making it particularly suitable for the reconstruction of a surface from a very large point set.
Keywords: *neural networks; growing cell structures; surface reconstruction; mesh generation; shape modeling.*

1 Introduction

Neural Network is a general term describing machines designed as a set of interconnected *nodes*, each one of which can store and process some information. The nodes communicate with the neighboring nodes, receiving and transmitting information with connections called synapses. Often, these connections also store some information, usually in the form of scalar weights.

The term Neural Network reflects some apparent similarities with the way the neural cells are interconnected in the human brain. Although, in principle, a neural network can be implemented as hardware, with real nodes and connections, in practice the most of the neural networks we use are simulated by the software.

A neural network can process the input data in several ways. For example, it can directly perform some computations, receiving an input signal, processing it on its nodes, and outputting the result, or it can be "trained" in a *learning process*. In the latter case the neural network processes the input signal by adjusting itself, and the state of the network is considered the output. The adjustment of the network during the learning process can include changes in the information stored on the nodes and the connections, as well as changes in the architecture of the network. That is, the network adapts its state to the input signals by creating new nodes and connections, or by pruning the existing ones.

The last two decades neural networks have found a lot of applications in such diverse areas, as pattern recognition, bio-informatics and finance, to mention only few of them. A typical application for a neural network, as for example the hand-writing recognition, is a simple problem which the human brain almost effortlessly solves, while the computer, despite its computational power, faces unexpected difficulties and requires sophisticated software for sometimes not very satisfactory results.

Here we use neural networks, in particular an adaptation of Fritzke's Growing Cell Structures, for mesh generation for surface reconstruction. Our results show that shape modeling is an area very well suited for the use of neural networks. Indeed, neural networks can give satisfactory answers in some challenging conditions, like the existence of sharp features, noisy data, or, very large scale data.

1.1 Related Work

The Neural Networks were introduced as a concept in the 40's, but the first practical applications started to emerge only in the last two decades. One of the main obstacles for their acceptance was that the software simulation of a neural network requires a computational power which only in the 80's was available. A comprehensive introduction into the mathematical theory of neural networks can be found in [3].

The last years there was a proliferation of Neural Network types, and the learning processes, that is, the way the Network adjusts to the input signals, can also be found in many different forms. One of the most widely used in practical applications is Kohonen's Self Organizing Maps [12]. A Self Organizing Map adjusts itself to the input signals,
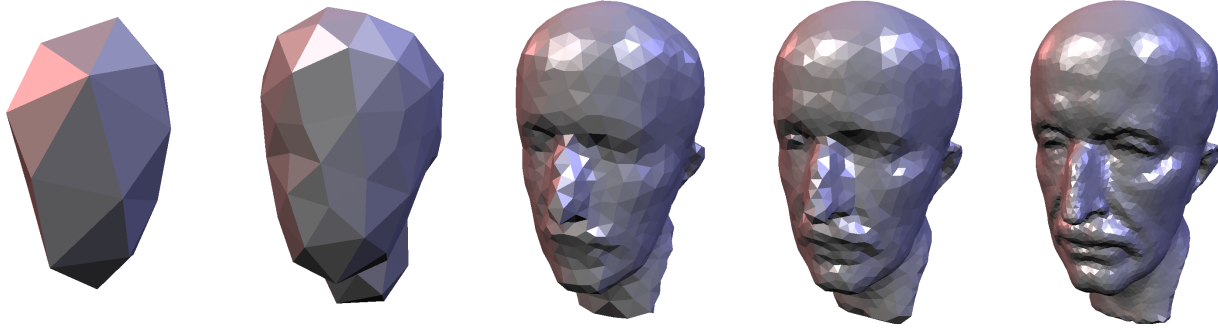
Figure 1. The Max-Planck model reconstructed incrementally from an unorganized cloud of 100K points. From left to right, the number of vertices of the constructed mesh is 20, 100, 1K, 2K and 8K.

learning gradually the space of the input data. It can reveal patterns of that input data space that the human brain cannot detect, either because of the nature of these data, like high dimensionality, or because of their size and complexity.

A similar approach to the Self Organizing Maps is the Growing Cell Structures of Fritzke [8]. A Growing Self Structure is a neural network that grows incrementally. We start with a very simple network, and, responding to the input signals we add new nodes, one by one. For a discussion on the incrementally growing networks, and their advantages over the non-incremental self-organizing networks, see [7].

Applications of the neural networks in Computer Graphics related problems include [18], where Self Organizing Maps were used in surface reconstruction, and [4], where the Growing Cell Structures are employed for Finite Element mesh generation. The [4] can also serve as an introduction to the Growing Cell Structures.

Although the Neural Networks is a powerful, emerging technology, and the investigation of its applicability in Computer Graphics problems has an interest by its own, we found that in many aspects our results are comparable with those of the established non-neural methods, like [10, 2, 13, 1, 15, 11, 5].

Finally, because of the intuitive character of the Neural Networks, most of their applications have a constant point of reference to some Physics related methods. In our case our work is similar in the spirit with the snakes and active surfaces [16, 17].

1.2 Motivation

Although many algorithms have already been proposed for mesh generation from an unorganized point cloud and for the polygonization of an implicit surface, there is still a lot of active research in this area, showing that there are still problems which have not been addressed properly.

For example, in mesh generation from a point cloud there are situations where many algorithms will not give a perceptually correct answer. In fact, most of the methods do not cope very well with sharp features and concavities, and require sophisticated modifications allowing them to detect such features and adapt. Another common source of problems is the size of the data set. Todays, data sets consisting of hundreds of millions of points are common, especially in cultural heritage projects like the Digital Michelangelo, and the most of the existing algorithms can not deal with such an amount of data.

The neural network approach, although it has some drawbacks itself, gives some interesting solutions to the above problems. As the input data set is not processed itself but it is only sampled, one point at a time, and given that the sampling process is not the bottleneck of our computations, we may assume that the time performance of the algorithm is practically independent of the size of the input data set. Also, our implementation of the Growing Cell Structures shows a particular flexibility, and we have found experimentally that it can handle satisfactory the sharp features and the concavities of the reconstructed surface. Finally, its stochastic nature makes it resilient to noisy or corrupted data.

1.3 Overview

Here, we give a brief description of one step of our version of the Growing Cells Algorithm. The network is our mesh, and its nodes are the mesh vertices. The information stored in a node is a 3-dimensional vector **v**, giving the position of that vertex, and a scalar value, called the *signal counter*, measuring the activity of that vertex during the learning process. The connections between the nodes correspond to the edges of the mesh and they do not carry any information other than connectivity.

In one step of the algorithm we sample our target space
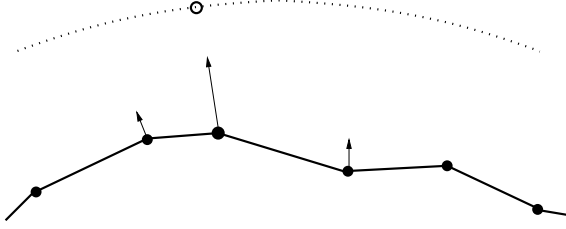
Figure 2. The target space $\mathcal{P}$ is denoted by the dotted line and the signal sampled from $\mathcal{P}$ by a circle. The current state of the network is denoted by the solid line. The best matching node, denoted here by the large disk, moves towards the signal while its direct topological neighbors also adjust their position.

$\mathcal{P}$, which is a point cloud or an implicit surface, thought here as a probability distribution. The sample is a single point s, seen here as a signal that will be processed by the neural network. We select the node of the network which is the nearest to the sample, and we move that node and its direct topological neighbors towards the sample. This way the nodes move towards the target space, adapting their position to its geometry, see Fig. 2. Then, we update the signal counters of the nodes, increasing the counter of the best matching node to reflect its recent activity. The fact that only the best matching node and its topological neighbors respond to a signal can be seen as a kind of competition between the nodes and, traditionally, this kind of process is called *competitive learning*.

After a certain number of iterations of the step described above, we perform some operations that change the size and the connectivity of the mesh. We split the most active vertices and we remove by an edge collapse the most inactive. The reason is that the most active vertices are near a part of $\mathcal{P}$ which is currently under-represented by the network, while the most inactive vertices are near a part of $\mathcal{P}$ which is over-represented by the network, or it even happens that these inactive vertices are totally misplaced. With these connectivity changing operations, the representation of the target space by the network improves and some previous mistakes are corrected.

The rest of the paper is organized as following. In Section 2 we describe in detail the Growing Cells Algorithm, following mainly [8], highlighting the modifications we propose to make it more suitable for the surface reconstruction problem. We also discuss in more detail the heuristic justification of the algorithm, explaining why it gives a good quality mesh representing fairly the reconstructed surface.

In Section 3 we experiment with different input data sets and we find that the algorithm copes particularly well with

the difficult situations described in 1.2.

2 The Growing Cell Algorithm for Surface Reconstruction

First we introduce some notation we will need in a more detailed description of the algorithm. As we mentioned above, the mesh generated by the algorithm is the neural network itself. Thus, for simplicity, both the neural network and the mesh will be denoted by $\mathcal{M}$. The set of the network nodes, as well as the set of vertices of the mesh will be denoted by $\mathcal{V}$. If $v \in \mathcal{V}$ is a vertex, the signal counter measuring its activity will be denoted by τ_v. If $\mathcal{M}$, is the mesh at a given stage of the algorithm, then the mesh after one step will be denoted by $\mathcal{M}'$, and the same notation will hold for the vertices and their signal counters. The target space that the network has to learn, thought here as a probability distribution in $\mathbf{R}^3$, will be denoted by $\mathcal{P}$. One point sampled from $\mathcal{P}$ will be denoted by s.

The main steps of the algorithm are the following:

1. Sample one point s from the target space $\mathcal{P}$.

2. Find the best matching node of the network (the *winner*), that is, find the vertex v_w of $\mathcal{M}$ with the shortest distance from s.

3. Update the position of v_w and its direct topological neighbors.

4. Update the signal counters of all the vertices of $\mathcal{M}$.

5. After a number of iterations of the above 1-4 steps, split the vertex with the highest signal counter.

6. After a number of iterations of the above 1-5 steps, remove the most inactive vertices of $\mathcal{M}$ with an edge collapse.

We explain each step in more detail:

1. The target space $\mathcal{P}$ is a point set, which can also be seen as a probability distribution. If $\mathcal{P}$ as point set is a point cloud, we make it a discrete uniform probability space by assigning to all the points an equal probability

$$\mathbf{p}(v) = \frac{1}{|\mathcal{V}|}, \quad v \in \mathcal{V} \tag{1}$$

If the target space is an implicit surface we assume that the distribution is uniform with respect to the area.

2. We use an octree-based searching tree to find the nearest neighbor of a given signal. Each node of the tree contains a bounding box of the vertices in the node, and it is split recursively when the number of vertices in the node exceeds a given constant. Since some of the vertices of $\mathcal{M}$ will change
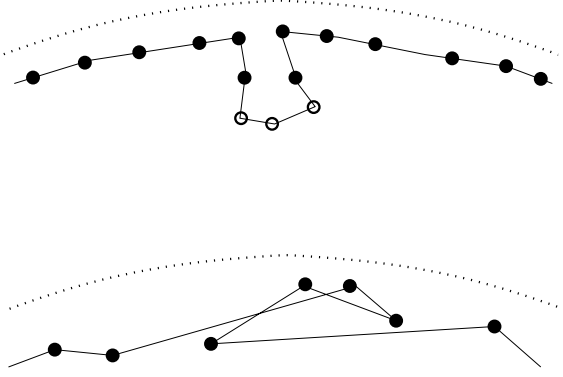
Figure 3. Up: The algorithm can converge towards a local minimum. The dotted line shows the target space. The solid line is the neural network. Notice that the three no-filled nodes can not be winners, nor one of their topological neighbors can. Therefore they will stay inactive. These local minima are resolved by the step 6 of the algorithm. Down: A fold-over may also occur. It is more difficult to be resolved, but a conservative strategy in the expansion of the network will prevent it.

position by step 3, the nodes of the tree should be updated on every iteration. Insertion or removal of a vertex is done only at the leaf level, and the updating of the tree is performed in $O(\log n)$ time, where n is the number of vertices of the final mesh. As each new vertex of the mesh inserted by step 5 requires a constant time of iterations of step 2, the total computational cost of step 2 is $O(n \log n)$.

3. The position of the best matching vertex v_w is updated as a linear combination of itself and the sample s

$$v'_w = (1 - \alpha_w)v_w + \alpha_w s \qquad (2)$$

where α_w is a constant. A relatively large value of α_w will increase the mobility of the vertices of the mesh and will make more probable the occurrence of some unwanted effects as convergence to local minima or fold-overs. See Fig. 3.

Notice that in a Self Organizing Map [12] the term α_w is a variable that tends to 0, guaranteeing the convergence of the algorithm. In contrast, in a Growing Cell Structure this term is constant and therefore, for any given number of nodes there is no convergence. Nevertheless, the algorithm converges as the number of nodes increases. Indeed, as the number of vertices of $\mathcal{M}$ increases, they cover $\mathcal{P}$ more densely, and the probability that the network's best matching vertex v_w is in the close vicinity of the sample s increases too.

At every step we also update the position of the topological neighbors of v_w. This is a balancing step performed in a way that will improve the distribution of vertices in the neighborhood of v_w for the given connectivity. For every v_i in the 1-ring of v_w we measure the Laplacian [14] $\mathcal{L}$ of v_i by

$$\mathcal{L}(v_i) = \frac{1}{\text{valence}(v_i)} \sum_{v_k \in 1-ring(v_i)} (v_k - v_i) \qquad (3)$$

and we update $\mathcal{M}$ by a fraction of the tangential component of $\mathcal{L}$

$$\mathcal{L}_t(v_i) = \mathcal{L}(v_i) - (\mathcal{L}(v_i) \cdot \mathbf{n})\mathbf{n} \qquad (4)$$

$$M' = M + \alpha_n \mathcal{L}_t \qquad (5)$$

where $\mathbf{n}$ is the approximated vertex normal of v_i, and α_n is a constant. This tangential smoothing of the topological neighbors of v_w is repeated a certain number of times, 5 in our implementation. It efficiently prevents fold-overs and convergence to local minima and also gives a fairer distribution of the vertices.

4. The signal counters of the vertices of the initial mesh are set to 0. After the processing of the sample s we update the signal counter of the v_w by

$$\tau'_{v_w} = \tau_{v_w} + 1 \qquad (6)$$

and then we decrease the signal counter of all the nodes by

$$\tau'_v = \alpha\tau_v, \quad v \in \mathcal{V} \qquad (7)$$

where α is a constant. The signal counters give an indication of how active is a node, that is, how many times it was the best matching node, with the most recent signals counting more than the older.

Notice that Eq. (7), although is just a single multiplication, still, introduces in the algorithm an element of $O(n^2)$ complexity. Also, notice that if c is the smallest integer such that

$$(1 - \alpha)^c = 0 \qquad (8)$$

in the machine's accuracy, then all the vertices that had not been best matches in the last c calls will have signal counter equal to zero. Therefore, in practice we only have to maintain a list of at most c vertices with non-zero signal counter to reduce the complexity to $O(n)$.

5. This step is called every λ iterations of the steps 1-4, where λ is a constant integer. First, we find the node with the highest signal counter. Then, we find the longest edge e adjacent to v_i and by traversing both directions equally we find the edges e_1, e_2 that split the star of v_i approximately at half, see Fig. 4. We perform the vertex split along e_1, e_2

positioning the new vertex at the middle of e. The signal counter of v_i is split between the two vertices proportionally to their Voronoi regions. We approximate the Voronoi region of a vertex by the square of the average length of the adjacent edges.
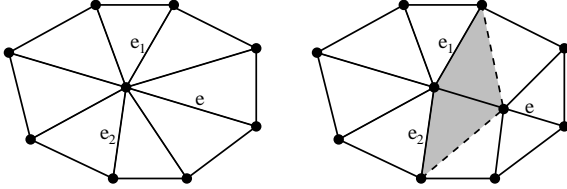
Figure 4. Left: A vertex of valence 8 has the largest signal counter and has to be split. Right: The vertex split is performed in a way that will distribute the valences as evenly as possible.

Intuitively, the signal counter measures the activity of a vertex, and the most active vertices are in an area of the target space $\mathcal{P}$ which is currently under-represented by the nodes $\mathcal{M}$. Thus, we perform a vertex split to create one more vertex in that area of $\mathcal{P}$.

6. This step of the algorithm is called every $\mu \cdot n$ iterations of the steps 1-4, where μ is constant integer and n the number of nodes of the network. Because of the machine accuracy problems caused by Eq. (7) we can not use the signal counter to find the less active nodes. Instead, we remove all the nodes that have not been active in the last $\mu \cdot n$ iterations of the steps 1-4. If the nodes of $\mathcal{M}$ are uniformly distributed in $\mathcal{P}$, then, in $\mu \cdot n$ calls of the steps 1-4 we expect a node v to be the winner μ times in average. The constant μ is a threshold beyond which, an inactive node will be considered misplaced and will be removed. The removal of the redundant vertices is done by an edge collapse. Since an edge collapse changes the valences of the incident triangles' vertices, we collapse the edge that gives the smallest regularity error, measured by

$$\frac{1}{3}\sqrt{(a+b-10)^2 + (c-7)^2 + (d-7)^2} \qquad (9)$$

where a, b, c and d are the valences of the vertices before the edge collapse, see Fig. 5.

These edge collapses are instrumental in improving the quality of the mesh. First they resolve most of the situations where the neural mesh converges towards a local minimum. In Fig. 3 the three totally inactive vertices will be deleted at some stage, exactly because they are totally inactive, resolving this way the local minimum. The second effect is that we remove vertices which are not so useful, in the sense that this part $\mathcal{P}$ is over-represented by the mesh.
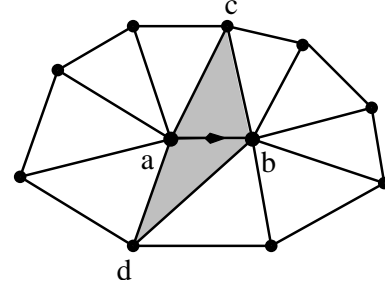
Figure 5. An edge with valence a, b ends collapses, creating a vertex of valence $a + b - 4$. The two vertices opposite to that edge had valences c, d before the collapse and have valences $c - 1, d - 1$ after.

The algorithm stops when some criteria are matched. Here we stop the algorithm after a certain number of nodes is reached.

2.1 Differences with the Growing Cell Structures

In the steps 1-4 of the algorithm the main difference with the original Growing Cell Structures, is the way the neighbors of the winning node v_w adjust their position. In [8] this is done as linear combination of the sample s and the position of the corresponding node, while here they are updated by a fraction of the tangential component of their Laplacian. Such an adjustment improves the quality of the mesh and prevents the surface from stacking to a local minimum or folding over.

The other difference is in the operations changing the connectivity of the mesh. In steps 5 and 6, we use vertex split and edge collapse, instead of edge split and vertex removal. These two operations, vertex split and edge collapse, which can be thought as inverse, are nearer to a Computer Graphics approach, see [9]. The advantage of the vertex split against the edge split, is that it tends to distribute more evenly the valences, improving the connectivity of the mesh, see Fig. 4.

The main advantage of an edge split, namely, that it easily generalizes into higher dimensions is not very relevant in our context.

The edge collapse, which complements the vertex split, is used here because it preserves the topology of the mesh, while a vertex removal may create boundaries and multiple connected components. As a result, using a topologically safe operation, we are able to employ a more aggressive strategy for the removal of the inactive vertices, improving this way the quality of the final mesh.

Using only topology preserving operations it also means

that the topology of the final mesh will be the same with the topology of the initial network. The adaptation of the algorithm so that it dynamically recognizes the topology of the target space, in the spirit of [6], is left as future work.

2.2 Performance related heuristics

Intuitively, the algorithm works by moving gradually the vertices of the network towards the target space $\mathcal{P}$. In our experiments we also noticed that the connectivity of the final mesh is usually very good. In a typical situation, about half of the vertices have valence 6, and only around 5% of the valences are different than 5,6,7, see Table 1. The good quality of the connectivity can also be confirmed by visual inspection of the wireframe view of the constructed meshes, see Fig. 6. Here we give some heuristic arguments, explaining why we expect the algorithm to give, in general, good quality meshes.
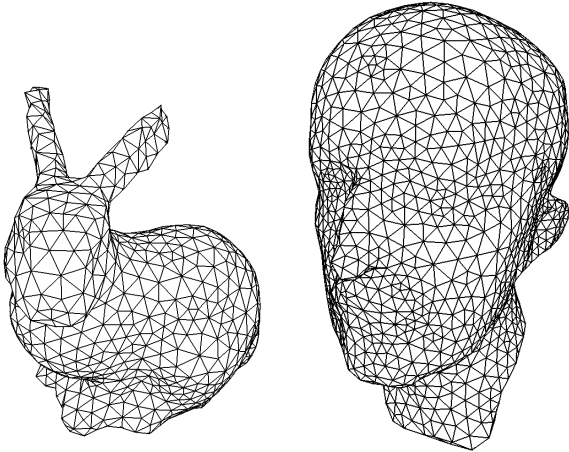
Figure 6. The wireframe view of the Bunny model with 1K vertices and the Max-Planck model with 2K vertices.

We notice that the target space $\mathcal{P}$ can be thought both as a probability distribution and as a smooth surface which is sampled. As the network converges to that surface, each triangle approximates a part of the probability distribution, and we can define an approximating probability measure on the triangles. This measure is equal to the probability that a random sample from $\mathcal{P}$ lies inside that triangle.

Intuitively, we expect that the probability measures of the triangles tend to become equal. Indeed, large probability measure means high probability that a sample is in the interior of that triangle, and the processing of such a sample will make the triangle to shrink, see Fig. 7. We expect that this intuitive claim can be rigorously proved with the
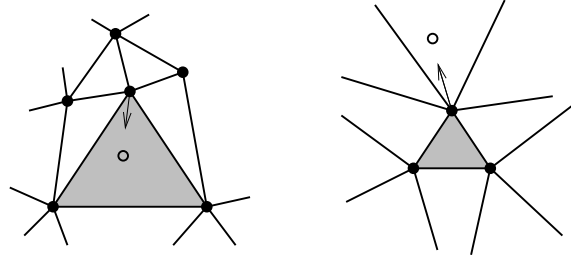
Figure 7. Left: A triangle with high probability measure (grey triangle) is more likely to be sampled in its interior and shrink as a result. Right: A triangle with low probability measure is more likely to expand as a result of a sample near to one of its vertices but outside the triangle.

standard mathematical theory of neural networks, but such a proof is beyond the scope of this paper.

As a consequence, if $\mathcal{P}$ is the uniform discrete probability on a point cloud, then the area of each triangle reflects the density of points at that part of $\mathcal{P}$. That is, we have many small triangles covering the parts of $\mathcal{P}$ with large concentration of points and few large triangles covering the areas where the points are sparse. If $\mathcal{P}$ is an implicit surface sampled uniformly with respect to its area, then the network will tend to have triangles of equal size.

Another important consequence is that the nodes with high valence are generally more active and there is a high probability that they will split, improving this way the connectivity of the network. Indeed, if the triangles have equal probability measure, then the probability measure of the Voronoi region around a high valence vertex, generally, will be greater than that of a low valence vertex. Fig. 8.

2.3 Discussion

When compared with the standard non-neural methods for surface reconstruction, one of the main differences of the above algorithm, is that the target space $\mathcal{P}$ is only sampled, one point at each step, and there are no calculations performed directly on $\mathcal{P}$. As a result the algorithm treats in a simple unified way different objects, such as point clouds, implicit surfaces, parametric surfaces, it is resilient to noisy or corrupted data and most importantly, its speed is not affected by the size of the data.

The algorithm treats the data in a very simple and basic way, that is, as stochastic signals. Many times this interpretation is quite near to the real nature of the data, as it is the case, for example, with the unorganized point clouds from scanned objects. And one may think of applications that re-
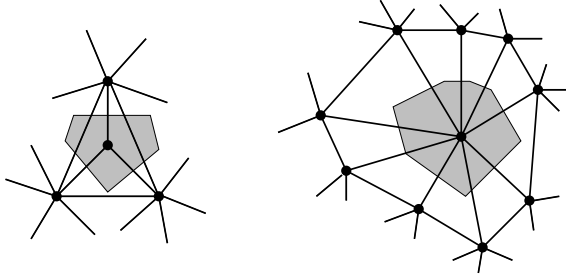
Figure 8. The high valence vertices are more active than the low valence vertices. The reason is that the Voronoi region of a vertex with high valence, generally, has greater probability measure than that of a low valence vertex. As a result the algorithm tends to split high valence vertices improving the connectivity of the mesh.

Table 1. Valence distribution for typical meshes. Notice that the distribution is almost independent from the shape of the model and the size of the constructed mesh.

		Valence				
	4	5	6	7	8	other
Sphere 1K	2	296	470	184	44	5
Bunny 1K	7	274	490	186	42	2
Max 2K	11	571	941	390	73	15
Teeth 2K	5	576	932	411	69	8
Sphere 5K	10	1451	2330	999	177	34
Bunny 5K	22	1416	2364	987	177	35
Dino 5K	24	1447	2307	1001	190	32
Teeth 5K	17	1481	2244	1043	189	27
Max 8K	36	2337	3652	1608	323	45

quire the use of such kind of neural algorithms because we can not express the data in any other form than that of a set of stochastic signals.

Regarding the drawbacks of the algorithm, the main one is the speed which, especially for small data sets, is lower than that of the most existing algorithms.

3   Examples

In this section we present the results of several experiments. We used the set of constants

$$\alpha_w = 0.06, \ \alpha_n = 0.05, \ \alpha = 0.95, \ \lambda = 100 \qquad (10)$$

that were experimentally found and proposed in [8]. Sometimes we used $\lambda = 70$ to speed up the process without noticing any side-effect. We used the value $\mu = 20$, but we do not claim that this value is optimal in any sense.

The initial mesh was always a tetrahedron and the final mesh a closed surface of genus 0. The result are shown at the end of the paper.

In the first experiment the target space is a sphere. It is defined implicitly and the sampling is almost uniform with respect to the area of the sphere. The other experiments were with point clouds obtained from some standard polygonal meshes. The Max-Planck model with 100K vertices is shown, in Fig. 1 in the beginning of the paper. The Stanford Bunny with 35K vertices, the dinosaur with 42K vertices, and the teeth with 116K vertices are shown at the end of the paper.

Table 1 gives the valence distribution for some of the reconstructed meshes, showing that the algorithm produces meshes with very good connectivity.

4   Conclusion and Future Work

We presented an adaptation of the Growing Cell Structures for surface reconstruction. Experimenting, we found that the algorithm works satisfactorily in many different situations, sometimes outperforming algorithms based on more transitional approaches, especially in issues related to mesh quality.

In the future we will adapt the algorithm so that it dynamically recognizes the topology of the input data space, and we will also try to find new applications for the algorithm presented here. In general, we think that there is a great scope for further investigation into novel applications of the Neural Networks in problems related to Computer Graphics and Scientific Visualization.

References

[1] N. Amenta, M. Bern, and M. Kamvysselis. A new voronoi–based surface reconstruction algorithm. In *SIGGRAPH 98, Conference Proceedings*, pages 415–422, 1998.

[2] C. L. Bajaj, F. Bernardini, and G. Xu. Automatic reconstruction of surfaces and scalar fields from 3D scans. In *SIGGRAPH 95, Conference Proceedings*, pages 109–118, 1995.

[3] C. M. Bishop. *Neural Networks for Pattern Recognition*. Oxford University Press, 1995.

[4] C.-A. Bohn. *Radiosity on Evolving Networks*. PhD thesis, Fachbereich Informatik, Universitat Dortmund, Dortmund, Germany, 2000.

[5] J. C. Carr, R. K. Beatson, J. B. Cherrie, T. J. Mitchell, W. R. Fright, B. C. McCallum, and T. R. Evans. Reconstruction and representation of 3d objects with radial basis functions. pages 67–76, 2001.

[6] B. Fritzke. A growing neural gas network learns topologies. In G. Tesauro, D. S. Touretzky, and T. K. Leen, editors, *Advances in Neural Information Processing Systems 7*, pages 625–632. MIT Press, Cambridge MA, 1995.

[7] B. Fritzke. Growing self-organizing networks – why? In *ESANN'96: European Symposium on Artificial Neural Networks*, pages 61–72, 1996.

[8] B. Fritzke. Growing cell structures - a self-organizing network for unsupervised and supervised learning. Technical Report ICSTR-93-026, International Computer Science Institute, Berkeley, May 93.

[9] H. Hoppe. Progressive meshes. In *SIGGRAPH 96 Conference Proceedings*, pages 99–108, 1996.

[10] H. Hoppe, T. DeRose, T. Duchamp, J. McDonald, and W. Stuetzle. Surface reconstruction from unorganized points. In *SIGGRAPH 92, Conference Proceedings*, pages 71–78, 1992.

[11] L. Kobbelt, J. Vorsatz, U. Labsik, and H.-P. Seidel. A shrink wrapping approach to remeshing polygonal surfaces. *Computer Graphics Forum*, 18(3):119–130, 1999.

[12] T. Kohonen. Self-organized formation of topologically correct feature maps. *Biological Cybernetics*, 43:59–69, 1982.

[13] V. Krishnamurthy and M. Levoy. Fitting smooth surfaces to dense polygon meshes. In *SIGGRAPH 96, Conference Proceedings*, pages 313–324, 1996.

[14] G. Taubin. A signal processing approach to fair surface design. In *SIGGRAPH 95, Conference Proceedings*, pages 351–358, 1995.

[15] M. Teichmann and M. Capps. Surface reconstruction with anisotropic density–scaled alpha shapes. In *IEEE Visualization 98, Conference Proceedings*, pages 67–72, 1998.

[16] D. Terzopoulos. Regularization of inverse visual problems involving discontinuities. *IEEE Transactions on Pattern Analysis and Machine Intelligence*, 8:413–424, 1986.

[17] D. Terzopoulos, J. Platt, A. Barr, and K. Fleischer. Elastically deformable models. In *SIGGRAPH 87, Conference Proceedings*, pages 205–214, 1987.

[18] Y. Yu. Surface reconstruction from unorganized points using self-organizing neural networks. In *IEEE Visualization 99, Conference Proceedings*, pages 61–64, 1999.
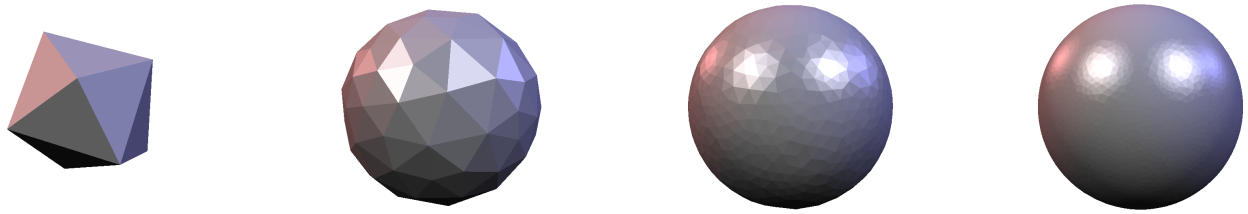
Figure 9. A sphere reconstructed from an implicit surface. The polygonal meshes have 10, 100, 1K and 5K vertices, corresponding.
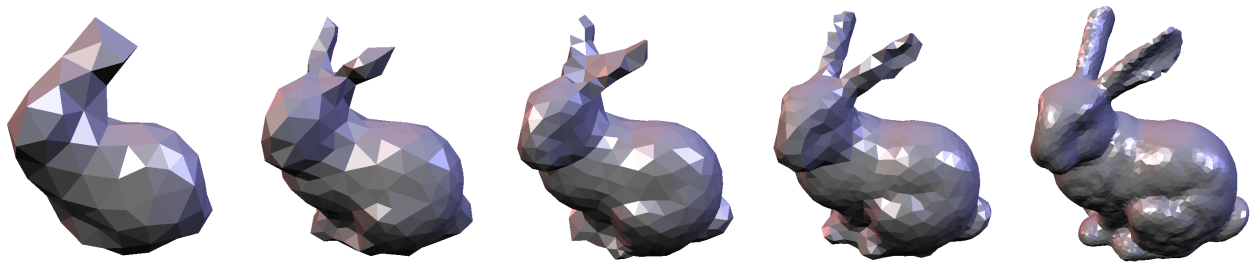

Figure 10. The Bunny with 100, 300, 500, 1K and 5K vertices, corresponding.

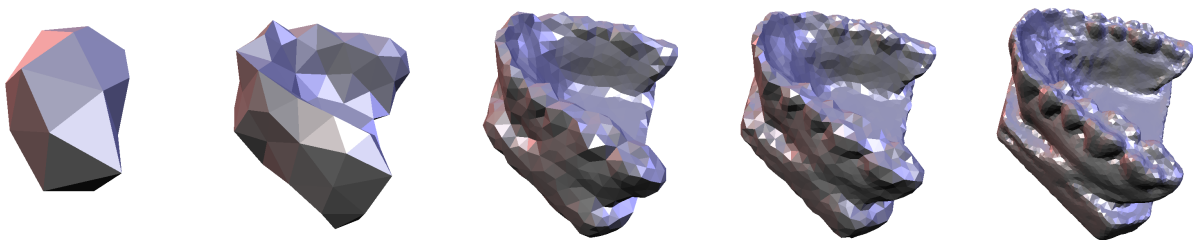**Figure 11. The Dinosaur with 100, 500, 1K, 1.5K and 2.5K vertices, corresponding.**

Figure 12. The teeth model with 20, 100, 1K, 2K and 10K vertices, corresponding.